



Published in final edited form as:

Br J Ophthalmol. 2019 July ; 103(7): 933–937. doi:10.1136/bjophthalmol-2018-312620.

Macular spatial distribution of preserved autofluorescence in patients with choroideremia

Amir H Hariri^{1,2}, Michael S Ip^{1,2}, Aniz Girach³, Byron L Lam⁴, M. Dominik Fischer⁵, Eeva-Marja Sankila⁶, Mark Edward Pennesi⁷, Frank G Holz⁸, Robert E Maclaren^{9,10}, David G Birch¹¹, Carel B Hoyng¹², Ian M MacDonald¹³, Graeme C Black¹⁴, Stephen H Tsang^{15,16}, Neil M Bressler¹⁷, Kimberly E Stepien¹⁸, Michael Larsen¹⁹, Michael B Gorin², Isabelle Meunier²⁰, Andrew R Webster^{21,22}, and Srinivas Sadda^{1,2} Natural History of the Progression of Choroideremia (NIGHT) Study Group

¹Doheny Image Reading Center, Doheny Eye Institute, Pasadena, California, USA ²Department of Ophthalmology, David Geffen School of Medicine of the University of California-Los Angeles, Los Angeles, California, USA ³Nightstar Therapeutics, London, UK ⁴Bascom Palmer Eye Institute, University of Miami Miller, School of Medicine, Miami, Florida, USA ⁵Centre for Ophthalmology, University of Tübingen, Tübingen, Germany ⁶Helsinki University Eye Hospital, Helsinki, Finland ⁷Casey Eye Institute, Oregon Health & Science University, Portland, Oregon, USA ⁸Department of Ophthalmology, University of Bonn, Bonn, Germany ⁹Nuffield Laboratory of Ophthalmology, Department of Clinical Neurosciences, University of Oxford and Oxford University Eye Hospital, NHS Foundation Trust, NIHR Biomedical Research Centre, Oxford, UK ¹⁰Moorfields Eye Hospital, NHS Foundation Trust, NIHR Biomedical Research Centre, London, Texas, USA ¹¹Retina

Correspondence to Dr Srinivas Sadda, Doheny, Eye Institute, Los Angeles, CA, 90033, USA; ssadda@doheny.org.

Contributors AHH and SS have full access to all the data in the study and takes responsibility for the integrity of the data and the accuracy of the data analysis. Study concept and design: AHH. Acquisition, analysis or interpretation of data: all authors. Drafting of the manuscript: AHH, SS. Critical revision of the manuscript for important intellectual content: all authors. Statistical analysis: AHH. Administrative, technical or material support: AG. Study supervision: SS.

Disclaimer AHH: No financial disclosures. MSI: Thrombogenics (Consultant), Boehringer Ingelheim (Consultant), Omeros (Consultant), Genentech (Consultant), Quark (Consultant). AG: Employee of Nightstar Therapeutics. BLL: Research funding from Nightstar Therapeutics. MDF: Nightstar Therapeutics (Consultant, Financial Support), Casebia Therapeutics (Consultant, Financial Support), Spark Therapeutics (Consultant), Regenxbio (Consultant), Eyeserve GmbH (Consultant), Bayer (Financial Support), Novartis (Financial Support). E-MS: No financial disclosures. MEP: No financial disclosures. FGH: Nightstar Therapeutics (Financial Support), Carl Zeiss Meditec (Financial Support), Optos (Financial Support), Allergan (Consultant, Financial Support), Roche/Genentech (Consultant, Financial Support), Alcon (Consultant), Novartis (Consultant/Financial Support), Bayer (Consultant/Financial Support), Boehringer-Ingelheim (Consultant), Centervue (Financial Support), Iin Bioscience (Consultant), Pixium (Consultant/Financial Support), Thrombogenics (Consultant). REM: Nightstar Therapeutics (Financial Support, Consultant, Founder and Director), Spark Therapeutics (Consultant) DGB: Nightstar Therapeutics (Consultant, Financial Support), Ionis Pharmaceuticals (consultant, financial support), Genentech (consultant), Nacuity (consultant), AGTC (consultant, financial support), 4D (financial support). CBH: No financial disclosures. IMM: Allergan (Consultant), Canadian Institutes for Health Research (Grant support), Alberta Innovates (Grant support), Foundation Fighting Blindness (Grant support). GCB: No financial disclosures. SHT: No financial disclosures. NMB: Alkeus; Bayer; Chiltern; Nighstar Therapeutics; Novartis; Roche Samsung Bioepis. KES: No financial disclosures. ML: No financial disclosures. MBG: No financial disclosures. IM: No financial disclosures. ARW: No financial disclosures. SS: Carl Zeiss Meditec (Consultant, Financial Support), Optos (Consultant, Financial Support), Allergan (Consultant, Financial Support), Genentech (Consultant, Financial Support), Alcon (Consultant), Novartis (Consultant), Iconic (Consultant).

Competing interests None declared.

Patient consent Obtained.

Ethics approval University of California, Los Angeles.

Provenance and peer review Not commissioned; externally peer reviewed.

This work was presented at 2018 ARVO annual meeting in Honolulu, HI, USA on 2 May 2018 as an oral presentation.

Foundation of the Southwest, Dallas, Texas, USA ¹²Department of Ophthalmology, Radboud University Medical Center, Nijmegen, The Netherlands ¹³Department of Ophthalmology and Visual Sciences, University of Alberta, Edmonton, Alberta, Canada ¹⁴Manchester Centre for Genomic Medicine, Central Manchester University Hospitals NHS Foundation Trust, Manchester Academic Health Sciences Centre, St Mary's Hospital, Manchester, UK ¹⁵Department of Ophthalmology, Columbia University, New York, USA ¹⁶Department of Pathology and Cell Biology, Columbia University, New York, USA ¹⁷Wilmer Eye Institute, Johns Hopkins University School of Medicine, Baltimore, Maryland, USA ¹⁸Department of Ophthalmology & Visual Sciences, Madison, Wisconsin, USA ¹⁹Department of Ophthalmology, Rigshospitalet and University of Copenhagen, Copenhagen, Denmark ²⁰Eye Clinic, Hôpital Robert Debré, CHRU de Reims, Reims, France ²¹Moorfields Eye Hospital NHS Foundation Trust, London, UK ²²UCL Institute of Ophthalmology, London, UK

Abstract

Background/Aims—To better understand the pattern of degeneration progression in cases with choroideremia.

Methods—A cohort of genotypically confirmed choroideremia cases who underwent optical coherence tomography (OCT) and fundus autofluorescence (FAF) imaging was studied. Using HEYEX review software, the foveal centre was marked on FAF images under guidance of corresponding OCT images, followed by application of an ETDRS grid. The boundaries of preserved autofluorescence (AF) were manually segmented in each individual ETDRS subfield. The regional distribution of preserved AF was assessed by comparing its area among the various subfields.

Results—A total of 168 eyes from 84 choroideremia cases were enrolled. There was a statistically significant difference in the amount of preserved AF area between inner subfields as determined by one-way analysis of variance ($F(3,668)=9.997, p<0.001$) and also between outer subfields ($F(3,668)=8.348, p<0.001$). A Tukey posthoc test revealed that the preserved AF area in the nasal subfields in both the inner and outer subfields was significantly smaller compared with analogue subfields.

Conclusion—The asymmetric spatial distribution of preserved AF in choroideremia (corresponding to the stellate shaped nature of these regions) suggests that the progression of degeneration has directional preference.

INTRODUCTION

Choroideremia as an X linked recessive, slowly progressive retinal degenerative disorder,¹ affects the retinal pigment epithelium (RPE), neurosensory retina and choroid.² Degenerative changes start from the periphery and expand centripetally.

Choroideremia is usually caused by null mutations in the CHM gene (Xq21), which leads to the absence of the intracellular protein, Rab escort protein-1.^{3,4}

There is no proven treatment for choroideremia yet but recently a pilot gene replacement therapy has been considered as a potential treatment approach for the disease.⁵⁶ This pilot study suggesting a possible improvement in visual acuity has triggered interest in expanding to larger trials and using outcome measures beyond visual acuity and prompted working on anatomical outcome measures in choroideremia. We recently reported on quantitative approaches for monitoring and measuring the progression of choroideremia.⁷ In this previous study, we observed that the configuration of the preserved outer retina and RPE, manifesting as preserved autofluorescence (AF) by fundus autofluorescence (FAF) imaging, varied considerably from cases to case and typically occupied an irregular, stellate shape, very different from many other retinal degenerations. This observation prompted us to investigate the pattern of progression of the outer retinal atrophy in choroideremia and to evaluate for potential differences in the directional shrinkage of preserved AF in choroideremia.

In the present study, we take advantage of a large longitudinal prospective natural history study of choroideremia to evaluate the macular spatial distribution of preserved AF in patients with choroideremia in order to gain better insight into the specific pattern of disease progression.

METHODS

Description of cohort

The design, inclusion and exclusion criteria and the participants in the natural history of the progression of choroideremia (NIGHT) study have already been described in detail.⁷

Briefly summarised for the purpose of this article, subjects with a confirmed genetic diagnosis of choroideremia were enrolled in this multicentre study. All participants underwent spectral domain optical coherence tomography (SDOCT) and FAF imaging at baseline using the Heidelberg Spectralis HRA+OCT (Heidelberg Engineering, Heidelberg, Germany) system. OCT imaging was performed using 30×25 degree field of view and a 5.9 mm×5.9 mm pattern size with an ART of 12 images averaged. FAF images were obtained using 488 nm ('blue peak') light and a 30 degree field of view, centred on the fovea. The analyses in this study were approved by the Institutional Review Board of the University of California, Los Angeles. The research adhered to the tenets set forth in the Declaration of Helsinki.

Grading protocol

The intragrader and intergrader reproducibility for segmenting areas of preserved AF (representing areas of preserved RPE) on FAF imaging have been demonstrated in a previous publication.⁷ In this study, one of these certified Doheny Image Reading Center (DIRC) senior graders performed all assessments. For each case, using the Heidelberg Eye Explorer (HEYEX) review software, the foveal centre was marked on the infrared reflectance image while simultaneously viewing the corresponding OCT. The ETDRS grid was then applied centred on the foveal centre (figure 1). These marked infrared reflectance images were then registered to the FAF images (figure 2). The boundaries of preserved AF

were manually segmented in each individual ETDRS subfield (figure 3). Areas of preserved AF were identified as well-demarcated regions of relative hyper autofluorescence (hyper AF) compared with the background areas of surrounding atrophy. To be included, islands of preserved AF were required to be at least 0.1 mm² in size and 175 μm in longest linear dimension.

Statistical analyses

To assess the regional distribution of preserved AF, the area of preserved AF was compared among the analogue subfields by 1-way analysis of variance (ANOVA) and Tukey posthoc tests. The correlation between the preserved AF areas of similar subfields in two eyes of the same subject was assessed using the Pearson correlation coefficient. For all the analyses, significance was set at $p < 0.05$. Statistical analyses were performed using commercial software (Statistical Package for Social Science V.19.0, SPSS, Armonk, New York, USA).

RESULTS

A total of 168 eyes from 84 cases of choroideremia received at the Doheny Image Reading Center from June 2017 to November 2017 were included in this analysis.

The mean of preserved AF area within the ETDRS subfields in all eyes was 5.25 ± 5.23 mm² (range: 0.1–26.72 mm²).

In 32 eyes, foveal centre subfield was completely preserved, and in 112 eyes the preservation was partial.

The means of preserved AF areas in the various ETDRS subfields are shown in figure 4.

There was a statistically significant difference in the amount of preserved AF area between inner subfields as determined by one-way ANOVA ($F(3,668) = 9.997$, $p < 0.001$). A Tukey posthoc test revealed that the preserved AF area in the inner nasal subfield was 0.42 mm² smaller than the inner temporal subfield (95% CI 0.22 to 0.61 mm²; $p < 0.001$), 0.25 mm² smaller than the inner inferior subfield (95% CI 0.05 to 0.44 mm²; $p = 0.008$) and 0.23 mm² smaller than the inner superior subfield (95% CI 0.04 to 0.43 mm²; $p = 0.012$). There was no statistically significant difference between the inner inferior and inner temporal ($p = 0.116$), inner inferior and inner superior subfields ($p = 0.999$) and inner temporal and inner superior subfields ($p = 0.081$).

Analogously, there was a statistically significant difference in the amount of preserved AF area between outer subfields as determined by one-way ANOVA ($F(3,668) = 8.348$, $p < 0.001$). A Tukey posthoc test revealed that the preserved AF area in the outer nasal subfield was 0.52 mm² smaller than the outer superior subfield (95% CI 0.23 to 0.82 mm²; $p < 0.001$), 0.46 mm² smaller than the outer temporal subfield (95% CI 0.17 to 0.76 mm²; $p < 0.001$) and 0.36 mm² smaller than the outer inferior subfield (95% CI 0.06 to 0.65 mm²; $p = 0.010$). There were no statistically significant difference between the outer inferior and outer temporal ($p = 0.789$), outer inferior and outer superior subfields ($p = 0.482$) and outer temporal and outer superior subfields ($p = 0.959$).

Table 1 shows the correlation between preserved AF areas in similar ETDRS subfields of the two eyes of the same subject.

DISCUSSION

In this analysis, we evaluated the macular spatial distribution of preserved AF in choroideremia cases. We observed that the amount of preserved AF in ETDRS macular subfields was smallest in nasal subfields. The asymmetric macular spatial distribution of preserved AF in choroideremia (corresponding to the stellate shaped nature of these regions) suggests that the progression of the degeneration in these cases has a directional preference. To the best of our knowledge, this is one of the very few studies that supports a directional difference in progression of the degeneration at the macula in choroideremia cases.⁸⁹ We denote this as supportive since our presumption is based on cross-sectional data. Longitudinal data would be needed to confirm this finding. The stellate-shaped preserved areas in choroideremia are distinctly different from many other retinal degenerations such as retinitis pigmentosa where preserved areas are circular or oval, suggesting a more uniform rate of progression in all directions. The stellate pattern is, however, also seen in retinal degenerations caused by dominantly inherited RPE65 mutations,¹⁰ which is an RPE specific gene and this pattern might therefore be a feature specific to RPE layer degenerations.

Understanding the directional variability of progression of choroideremia would be important for assessing the efficacy of therapeutic interventions. For example, if a therapy was applied locally (eg, delivery of genetic material or stem cells) near one sector of a region of preserved AF, it may be expected to have the greatest impact on that sector. If that particular sector happens to manifest faster or slower underlying progression, it may affect the interpretation of the results, particularly if single OCT B-scan-based quantitative approaches such as measurement of EZ width are used.¹¹¹² In addition, as choroideremia is generally a slowly progressive disorder, recognising regions of faster progression may be important, as they may prove to be the best targets for locally acting therapies such as gene therapy. Also, recognising regions of faster progression in slowly progressive disorders may eliminate the necessity for longer follow-ups that are needed for detection of the significant changes in clinical trials.

The mechanism of this presumptive nasal macular directional preferential progression of the degeneration in choroideremia, yielding these stellate shapes of preserved AF, is uncertain. The finding that there is less preserved AF area nasally suggests that the nasal region may be more vulnerable to degeneration. We have speculated as to whether there may be regional anatomic variations in the outer retina and/or choroid that make these areas more vulnerable. For example, it is known that the choroid is thinner in the nasal ETDRS subfields.¹³ These areas that have a thinner choroid may precede the areas with thicker choroid in manifesting loss of the overlying RPE and retina as the overall degeneration progresses. An alternative explanation could be that the thinner areas of choroid provide less blood supply, and hence those areas of retina with thinner choroid are much more vulnerable to degeneration.

Normative studies of outer photoreceptor layer thickness have shown that the RPE-Outer Segment complex thickness in the superior macula, 0.5–3 mm from the foveal centre, was

significantly increased compared with the corresponding inferior retina.¹⁴ In our study, there was no statistically significant difference between the preserved AF area in superior and inferior macula. Thus, anatomic variation in ellipsoid zone and/or RPE layer does not seem to be related to the presumed directional preferential progression of the degeneration in choroideremia.

Previously, it has been reported that there was a strong correlation between the preserved AF areas of two eyes of the same subject.⁷¹⁵ In the present analysis, we also observed a correlation between preserved AF areas within the individual ETDRS subfields of the two eyes of the same subject (except for the outer nasal subfield). This suggests that directional preferential progression is similar in the two eyes and may have important implications in case the fellow eye is used as a control in choroideremia therapeutic trials.

Our study has some limitations which should be considered. First, this is a cross-sectional analysis of baseline data, and thus, we do not directly measure the directional progression rate of the degeneration in choroideremia cases. The directionality is only presumed based on the stellate-shape and the variable preservation in the various subfields. However, in a longitudinal study two sessions of grading of preserved AF areas in small ETDRS subfields significantly increase the grading noise, thus in such a slowly progressive degeneration a very long follow-up is needed to have a differential progression rate big enough to overcome the grading noise. Second, this study only evaluates the outer retinal degeneration (reflected by the FAF) associated with choroideremia and not the underlying associated choroidal degeneration. Without evaluating corresponding indocyanine green angiography or OCT angiography images, we cannot determine whether the choroidal degeneration follows a similar course.

On the other hand, this study has some strengths, including the collection of a relatively large cohort for an uncommon retinal disease. Another strength is the use of a trained, certified reading centre grader who was the senior grader for the previous study that demonstrated high levels of intergrader and intragrader reproducibility for FAF assessments in choroideremia cases.

In summary, the asymmetric macular spatial distribution of preserved AF in choroideremia (corresponding to the stellate shaped nature of these regions), while limited by its cross-sectional rather than longitudinal design, suggests that the progression of the macular degeneration in these cases has directional preference. This pattern could have implications for the design of anatomic endpoints for choroideremia clinical trials.

Acknowledgements

Nightstar Therapeutics is the sponsor of the Natural History of the Progression of Choroideremia (NIGHT) Study Group. Support for the reading center personnel was also provided in part by Beckman Macular Degeneration Research Center and a Research to Prevent Blindness Physician Scientist Award.

Funding The authors have not declared a specific grant for this research from any funding agency in the public, commercial or not-for-profit sectors.

REFERENCES

1. van den Hurk JA, Schwartz M, van Bokhoven H, et al. Molecular basis of choroideremia (CHM): mutations involving the rab escort protein-1 (REP-1) gene. *Hum Mutat* 1997;9:110–7. [PubMed: 9067750]
2. Jacobson SG, Cideciyan AV, Sumaroka A, et al. Remodeling of the human retina in choroideremia: rab escort protein 1 (REP-1) mutations. *Invest Ophthalmol Vis Sci* 2006;47:4113–20. [PubMed: 16936131]
3. Seabra MC, Brown MS, Goldstein JL. Retinal degeneration in choroideremia: deficiency of rab geranylgeranyl transferase. *Science* 1993;259:377–81. [PubMed: 8380507]
4. Cremers FP, van de Pol DJ, van Kerkhoff LP, et al. Cloning of a gene that is rearranged in patients with choroideraemia. *Nature* 1990;347:674–7. [PubMed: 2215697]
5. MacLaren RE, Groppe M, Barnard AR, et al. Retinal gene therapy in patients with choroideremia: initial findings from a phase 1/2 clinical trial. *The Lancet* 2014;383:1129–37.
6. Edwards TL, Jolly JK, Groppe M, et al. Visual acuity after retinal gene therapy for choroideremia. *N Engl J Med* 2016;374:1996–8. [PubMed: 27120491]
7. Hariri AH, Velaga SB, Girach A, et al. Measurement and reproducibility of preserved ellipsoid zone area and preserved retinal pigment epithelium area in eyes with choroideremia. *Am J Ophthalmol* 2017;179:110–7. [PubMed: 28499705]
8. Jolly JK, Edwards TL, Moules J, et al. A qualitative and quantitative assessment of fundus autofluorescence patterns in patients with choroideremia. *Invest Ophthalmol Vis Sci* 2016;57:4498. [PubMed: 27750291]
9. Jolly JK, Xue K, Edwards TL, et al. Characterizing the natural history of visual function in choroideremia using microperimetry and multimodal retinal imaging. *Invest Ophthalmol Vis Sci* 2017;58:5575–83. [PubMed: 29084330]
10. Bowne SJ, Humphries MM, Sullivan LS, et al. A dominant mutation in RPE65 identified by whole-exome sequencing causes retinitis pigmentosa with choroidal involvement. *Eur J Hum Genet* 2011;19:1074–81. [PubMed: 21654732]
11. Birch DG, Locke KG, Wen Y, et al. Spectral-domain optical coherence tomography measures of outer segment layer progression in patients with X-linked retinitis pigmentosa. *JAMA Ophthalmol* 2013;131:1143–50. [PubMed: 23828615]
12. Hariri AH, Zhang HY, Ho A, et al. Quantification of ellipsoid zone changes in retinitis pigmentosa using en face spectral domain-optical coherence tomography. *JAMA Ophthalmol* 2016;134:628. [PubMed: 27031504]
13. Ouyang Y, Heussen FM, Mokwa N, et al. Spatial distribution of posterior pole choroidal thickness by spectral domain optical coherence tomography. *Invest Ophthalmol Vis Sci* 2011;52:7019–26. [PubMed: 21810980]
14. Christensen UC, Kroyer K, Thomadsen J, et al. Normative data of outer photoreceptor layer thickness obtained by software image enhancing based on Stratus optical coherence tomography images. *Br J Ophthalmol* 2008;92:800–5. [PubMed: 18523085]
15. Aylward JW, Xue K, Patrício MI, et al. Retinal degeneration in choroideremia follows an exponential decay function. *Ophthalmology* 2018;125:1122–4. [PubMed: 29580667]

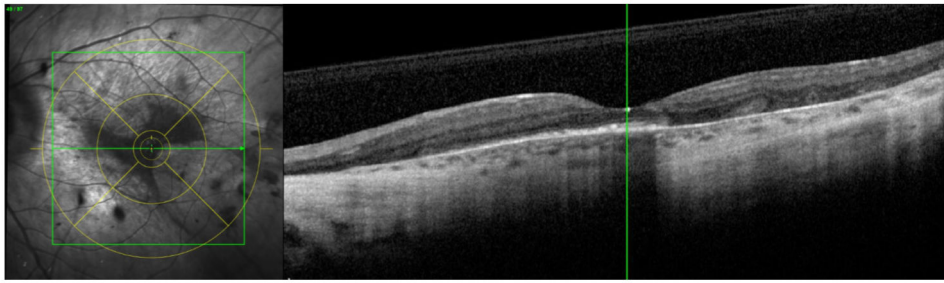


Figure 1. Taking advantage of Heidelberg Eye Explorer (HEYEX) review software, the foveal centre was marked on infrared reflectance images under the guidance of corresponding optical coherence tomography scans in every case, followed by application of an ETDRS grid.

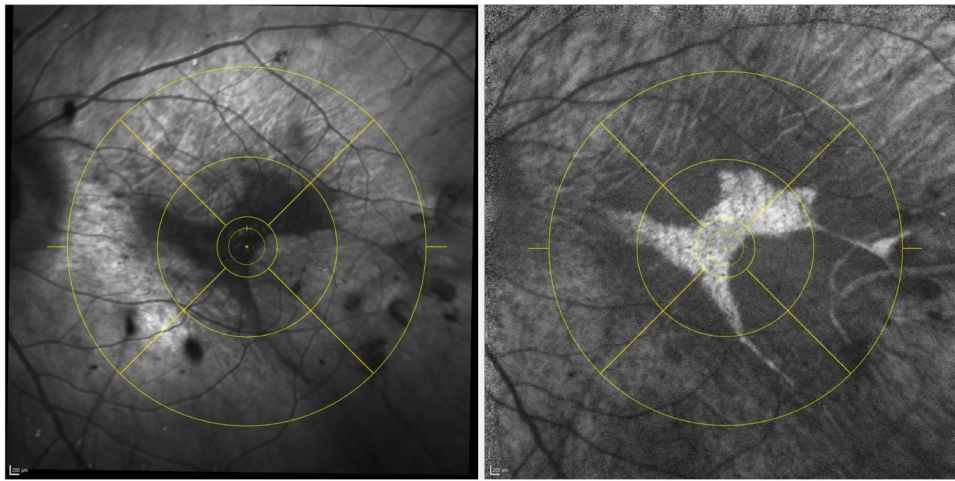


Figure 2. All infrared reflectance images with ETDRS grid (left panel) were registered to the fundus autofluorescence images (right panel).

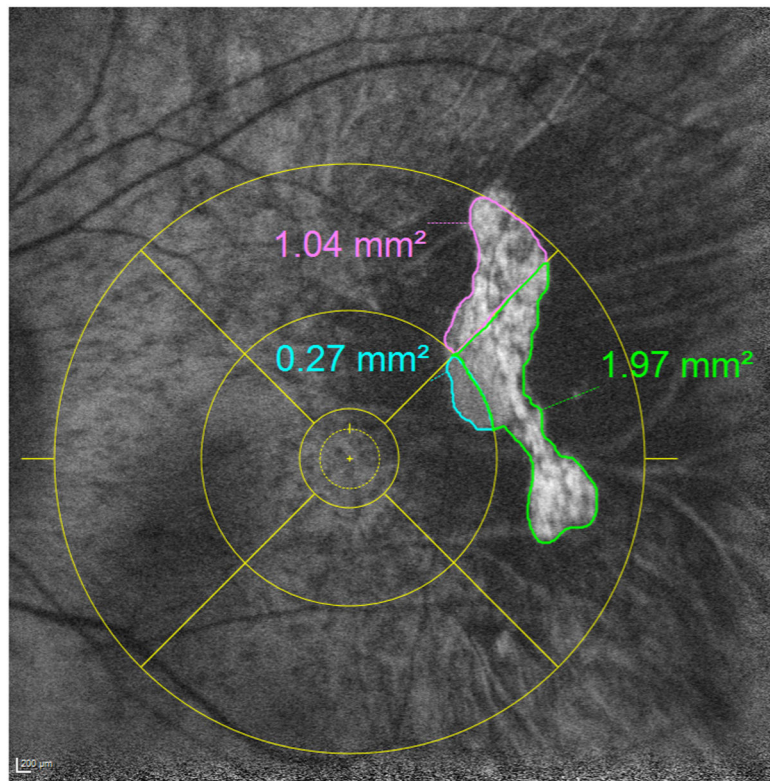


Figure 3.
The boundaries of preserved autofluorescence were manually segmented in each individual ETDRS subfield separately.

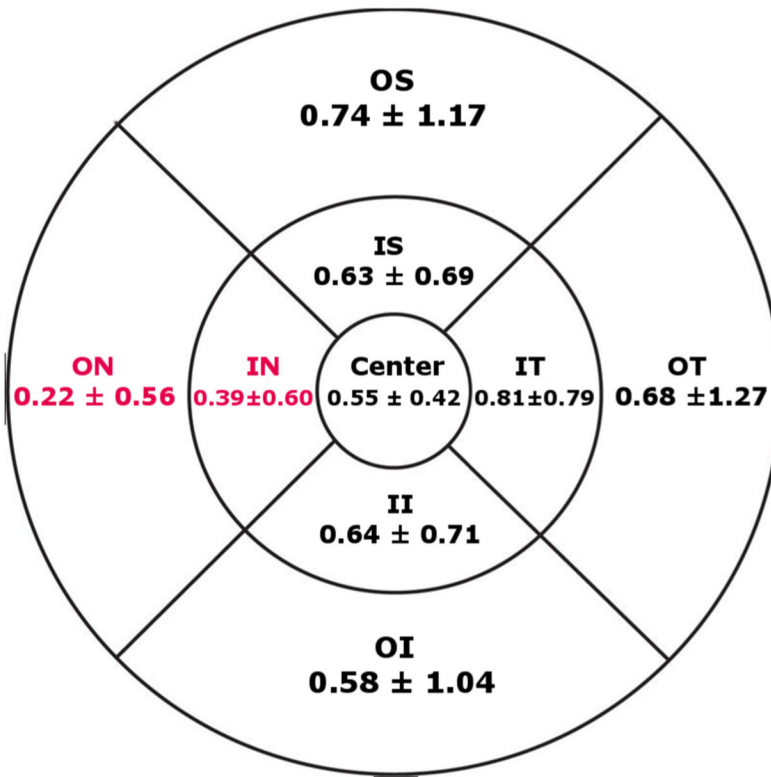


Figure 4. The average of preserved autofluorescence areas in different ETDRS subfields in mm².

Correlation between PAF areas in similar ETDRS subfields of the two eyes of the same subject

Table 1

ETDRS subfield	PAF area (Right eye)	PAF area (Left eye)	Correlation	95% CI		P value
				Upper	Lower	
Centre	0.56±0.42 *	0.54±0.43	0.71	0.59	0.80	<0.001
Inner nasal	0.35±0.60	0.44±0.60	0.59	0.43	0.71	<0.001
Inner inferior	0.64±0.69	0.64±0.72	0.73	0.61	0.82	<0.001
Inner temporal	0.79±0.79	0.83±0.78	0.66	0.52	0.77	<0.001
Inner superior	0.61±0.69	0.65±0.69	0.69	0.56	0.79	<0.001
Outer nasal	0.20±0.54	0.24±0.57	0.35	0.15	0.53	<0.001
Outer inferior	0.57±0.98	0.58±1.10	0.72	0.60	0.81	<0.001
Outer temporal	0.65±1.15	0.72±1.38	0.71	0.59	0.80	<0.001
Outer superior	0.79±1.25	0.69±1.09	0.67	0.53	0.77	<0.001

* All areas are in mm².

PAF, preserved autofluorescence.